https://doi.org/10.46813/2024-150-034

RESIDUA STRESSES AND DEFORMATION MECHANISMS IN THE SURFACE LAYER OF AA1933 ALUMINUM ALLOY INDUCED BY HIGH-CURRENT PULSED ELECTRON BEAM

V.V. Bryukhovetsky[1], V.V. Lytvynenko[1], D.E. Myla[1], V.V. Shatov[1], A.G. Ponomarev[2], O.L. Rak[2], V.A. Bychko[3]
[1]Institute of Electrophysics and Radiation Technologies NAS of Ukraine, Kharkiv, Ukraine
E-mail: ntcefo@yahoo.com;
[2]NSC "Kharkov Institute of Physics and Technology", Kharkiv, Ukraine;
[3]Chernihiv Polytechnic National University, Chernihiv, Ukraine

The purpose of the present study was to find out and show that rapid solidification of the surface layer of AA1933 aluminum alloy melted by irradiation with a high-current pulsed electron beam leads to the development of deformation processes in this layer. This results from thermo-elastic internal stresses arising during irradiation of the alloy with a pulsed electron beam. The value of residual internal stresses in the irradiation-remelted layer is 43 MPa. Since it is impossible to determine the deformation mechanisms during cooling of the remelted layer by direct methods, conclusions about the deformation mechanisms were made by studying the relief of the irradiated surface. This study shows that deformation processes during irradiation of AA1933 aluminum alloy can develop in different parts of the irradiated surface by different mechanisms. Deformation can be carried out by both dislocation slip and grain-boundary slipping mechanisms.

PACS: 29.25.Bx, 61.80.Fe, 62.20.−x

INTRODUCTION

Surface modification techniques such as the application of hard and wear-resistant coatings, surface treatment with concentrated energy flows, and saturation of the surface with metal and gas atoms are often used to improve the performance characteristics of aluminum alloys. Among the mentioned sources of concentrated energy flows, high-current pulsed electron beams (HPCEB), which were initially created for problems of plasma electronics and new acceleration methods, deserve special consideration [1, 2]. In recent decades, this tool has proven itself, among other things, as an effective method for modifying the surface of materials [3–5]. Such treatment allows to reduce the surface roughness of the material and increases its physical-mechanical, electro physical, and tribological characteristics [4–9]. Irradiation by HPCEB induces many interesting phenomena related to thermal and stress fields. Studies [4, 9] show that sharply non-equilibrium processes occur on metal surfaces, as a result of which metastable states can arise in surface layers, which are the source of improved physical, chemical, and mechanical properties unattainable using traditional surface treatment methods. Therefore, HCPEB methods draw more and more attention while discussing different options for surface modification of materials. Unlike conventional surface treatment methods, modification of material by HPCEB allows high-density energy to be released at a shallow depth from the material surface in a short time. Such irradiation causes rapid heating and cooling with a high-temperature gradient, resulting in melting, vaporization, plasma ablation, and the formation of thermal stresses and shock waves. As widely noted in many studies [3–9], the surface morphology of solids can change significantly after irradiation with HPCEB. At the same time, the morphological features of the surface are important and sometimes decisive for surface treatment and in some cases may limit the use of HCPEB as a new surface treatment method. However, a comprehensive understanding and detailed description of the processes occurring during HCPEB irradiation is still lacking.

The presence of strong residual internal stresses in coatings, which play a significant role in the kinetics of formation and fracture is a characteristic feature of most coatings produced by the pulsed electron beam method [10–13]. In many cases, such stresses present in the remelted layer play a positive role, contributing to the formation of a dense phase of the surface layer of the material, and preventing the emergence of inhomogeneities and macro-defects such as cracks and cavities. The stress-strain state of the material largely depends on the nature of relaxation processes developing after the impact of external factors. Relaxation effects are crucial both for the study of the structure of materials and for the scientific explanation of many of their intrinsic properties. The concept of relaxation as a process of motion of the system in the direction of thermodynamic equilibrium makes many essential contributions to revealing the physical picture of the stressed state of a solid body. In particular, recent experimental data have shown that even a single crystal of aluminum, which is not normally associated with strain twin formation, will twin when irradiated by HPCEB with properly specified parameters [12, 13]. These studies suggest that the high stress and strain rates induced by rapid heating and cooling due to irradiation by HPCEB can induce simultaneous displacement of entire atomic planes. In addition, some slip systems may be suppressed by thinning of the surface layer, which may contribute to strain twin formation. At present, there are no numerical calculations of the stress-strain state of the layer irradiated by HPCEB. This is due to both the heterogeneity of physical and technological properties of such layers and the lack of experimental studies of the surface relief of irradiated layers. Since it is impossible to determine the deformation mechanisms during cooling of the remelted layer by direct methods, it is possible to conclude the deformation mechanisms by studying the surface relief of the irradiated surface. Therefore, in this study, an attempt was made to describe possible mechanisms of deformation in the surface layer of the alloy based on the study of morphological features of the irradiated surface of AA1933 aluminum alloy, developing as a result of thermos-elastic stresses induced by HPCEB irradiation.

MATERIAL

High-strength alloys of the Al-Zn-Mg-Cu system, which includes the 1933 alloy, are of special interest in terms of aviation engineering development [14]. These alloys have high specific strength and at the same time are processable for the manufacture of deformed semi-finished products. The use of different heat treatment modes makes it possible to control the complex of their service characteristics in a wide range to the required operating conditions. At present, high-strength aluminum 1933 alloy is one of the main structural materials of modern aircraft. The studied AA1933 alloy has the following chemical composition: Al; 1.6…2.2 wt.%Mg; 0.8…1.2 wt.%Cu; 0.1 wt.%Mn; 0.66…0.15 wt.%Fe; 0.1 wt.%Si; 6.35…7.2 wt.%Zn; 0.03…0.06 wt.%Ti; 0.05 wt.%Cr; 0.10…0.18 wt.%Zr; 0.0001…0.02 wt.%Be. AA1933 is a high-strength alloy. The tensile strength σ_t of AA1933 alloy is 450…520 MPa [14]. The micro-hardness of alloy 1933 studied in this paper in the initial state is 105*HV*0.50. The micro-hardness of the HCPEB-irradiated layer of 1933 alloy, as previously found in [15, 16], is 137*HV*0.50. The alloy shows superplastic properties at high temperatures [17]. At temperature $T = 793$ K and true strain rate $\dot{\varepsilon} = 1.2 \cdot 10^{-4}\ s^{-1}$ elongation of samples of this alloy before fracture is 260% [17].

EXPERIMENTAL

Plates with a size of 100×100 mm were cut from the sheets of AA1933 alloy with a thickness of 2.5 mm for irradiation. The cladding layer on the plate surface was grinded off, and the plate surface was polished before irradiation. Irradiation of alloy sheets was performed by a HCPEB at the TEMP-A accelerator in the NSC KIPT of the NAS of Ukraine [15, 16]. The energy flux density at the target W is approximately 10^9 W/cm^2 (beam energy E ~ 0.35 MeV, current I ~ 2000 A, pulse duration $\tau_i \sim 5 \cdot 10^{-6}$ s, beam diameter ~ 3 cm). Irradiation was done by the single impulse in a vacuum at $1.3 \cdot 10^{-3}$ Pa.

Structural and topographic studies were performed using an *Olympus GX51* optical microscope and a JEOL JSM-840 scanning electron microscope. The phase composition of the alloy and determination of lattice parameters were studied by diffractometric analysis using X-ray diffractometer DRON-4. Diffractograms were obtained using filtered CuK_α-radiation at tube voltage $U = 40$ kV and current strength $I = 10$ mA. Profiles of diffraction maxima were plotted point by point at scanning step for $2\theta = 0.1°$ at the background and 0.01° at the maximum.

RESULTS AND DISCUSSION

Irradiation by HPCEB rapidly heats the material to a high temperature that significantly exceeds the melting point of aluminum alloys [1–3, 18]. Under the conditions of HCPEB action, the alloy heating rate is greater in the deep layers. The maximum energy absorption occurs at a depth of about 1/3 of the electron path in a given substance [18]. This leads to the explosive release of part of the molten material and subsequent rapid cooling of the alloy by heat dissipation into the main volume of the target. Cooling is accompanied by crystallization of molten material and structural-phase transformations.

Fig. 1 shows a general view of the surface of a target made of 1933 alloy sheet that has been irradiated by HPCEB. It can be seen that the intense thermal heating of the plate created by the electron beam led to the melting of its surface layer.

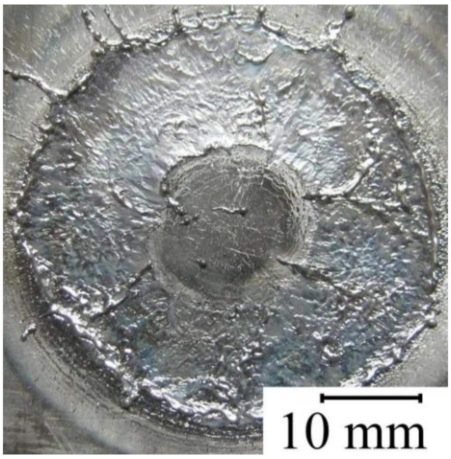

Fig. 1. General view of the surface of the AA1933 alloy plate irradiated by HPCEB

The features of structural and phase changes in the surface layer of industrial aluminum alloy AA1933 irradiated by HCPEB were studied earlier in [15, 16]. In particular, it was found that the action of a pulsed electron beam is accompanied by the formation of a distinct relief on the surface of the AA1933 alloy plate and the appearance of microcracks and craters on it.

Fig. 2 shows a view of a series of surface fragments of the AA1933 alloy plate after HCPEB irradiation. The specimen in this figure is not ground and retains a regular surface relief that records the crystallization and cooling history of its surface. It can be seen that the action of the pulsed electron beam is accompanied by the formation of a developed surface relief and the appearance of microcracks (see Fig. 2,b) and craters (see Fig. 2,c).

The crack formation seems to be caused by the action of thermos-elastic stresses during rapid crystallization of the surface molten by HCPEB. Cracking of the surface layer indicates the presence of significant internal stresses occurring in the melted layer at the time of its crystallization. As shown in Fig. 2,b, the cracks have zigzag sections. Zigzag crack propagation is probably related to local heterogeneity of strength characteristics and plasticity of the remelted layer in its various micro volumes and, in particular, to local heterogeneity of alloying elements distribution in the surface layer material during its crystallization. The relaxation of internal stresses resulting from the irradiation effect on the plate surface was not fully carried out during the crystallization of the melted surface layer, so the remaining internal stresses caused the formation of cracks.

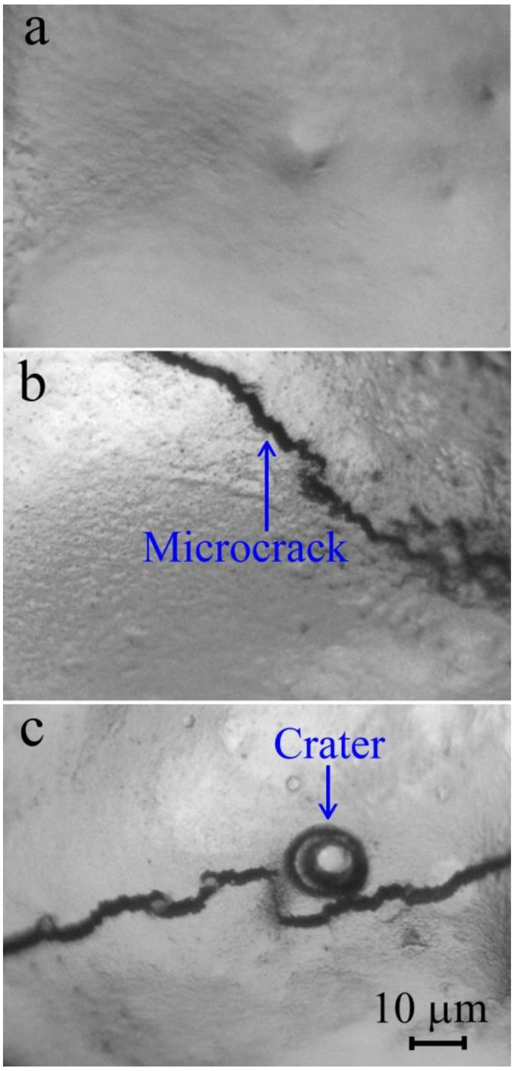

Fig. 2. Characteristic types of microstructure of fragments of HCPEB-irradiated AA1933 alloy surface

Crater formation is also observed on the irradiated surface (see Fig. 2,c). A detailed study of the types and characteristics of craters formed as a result of irradiation of AA1933 alloy by HCPEB was carried out earlier in [19]. It is believed that the formation of craters on the irradiated surface is one of the major adverse effects caused by HCPEB treatment. This is usually regarded as a deterioration of the physical and technological properties of the surface [20]. It is noted that an increase in surface roughness and formation of localized areas with highly non-uniform strain-stress state in the near-surface layer are the consequences of crater formation. However, under proper processing conditions, craters can be used to remove impurities in the surface layer through what is known as the "selective cleaning" effect, which can improve surface corrosion resistance [18]. Thus, studying the phenomenon of crater formation and evolution during HCPEB irradiation is extremely important to maximize the potential of the HCPEB method. Inhomogeneous local melting in the near-surface layers of the target material during irradiation and subsequent release of molten material through the hard outer surface is the main hypothesis of crater formation during HCPEB treatment among researchers [21]. The study [22] suggests a mechanism according to which the formation of craters is caused by the non-uniform crystallization of the surface layer molten by HCPEB. There are other opinions regarding the mechanism of crater formation [23].

As mentioned above, the presence of residual stresses, that is, internal stresses that exist in the material after the elimination of external influence, is an important factor affecting many physical and mechanical properties of metallic materials. Such stresses may also be the result of exposure of the material to streams of charged particles of different nature, including electrons. The occurrence of internal stresses can be associated with structural-phase changes occurring in the material in the area of direct impact by the charged particle streams and in the adjacent areas of the material. The unsteady temperature field arising in the surface layer of the target material as a result of beam energy absorption and the stress field caused by inhomogeneous heating of the object are the main factors determining the state and properties of the HCPEB impact zone [10, 11].

The determination of internal stresses by X-ray diffractometry is based on the experimental measurement of the relative change in interplanar distances, called lattice strain, and, assuming that this strain is elastic, the calculation of stress values according to Hooke's law [24].

Earlier in [15, 16] X-ray diffraction and micro-X-ray spectral analysis allowed to find out the peculiarities of the structural-phase state of initial and irradiated samples of AA1933 alloy. The initial microstructure of the studied alloy is characterized by the presence of Al_2CuMg, $MgZn_2$, and $Mg_3Zn_3Al_2$ phases, which play a significant role in the hardening of AA1933 alloy during its heat treatment. These phases are absent in HCPEB-irradiated samples. That is, the solid solution of the surface layer remelted by irradiation is enriched with zinc, copper, and magnesium atoms. Since the atomic radii of Zn and Cu are smaller than those of aluminum, saturation of the aluminum matrix with these elements should lead to a decrease in the lattice parameter. However, enrichment of the aluminum matrix with magnesium on the contrary should lead to an increase in the lattice parameter, since 1 at.% magnesium in pure aluminum increases the lattice parameter by 0.00046 nm. Taking into account the composition of the alloy, the total enrichment of the solid solution with these elements should not have a significant effect on the change of the crystalline alloy lattice parameter.

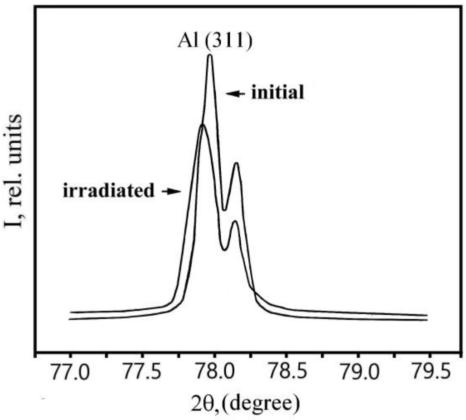

Fig. 3. (311) diffraction peaks for AA1933 aluminum alloy initial and irradiated samples

Fig. 3 shows the XRD curves that represent the diffraction peaks of the Al (311) atomic plane obtained from the surfaces of the AA1933 aluminum alloy sample surfaces of the original and 1 pulse HCPEB-irradiated aluminum alloy sample, respectively. Based on [24], the deformation values (ε) can be estimated from the relation:

$$\varepsilon = \frac{d_i - d_0}{d_0} \quad , \qquad (1)$$

where d_i – lattice period of Al in the plane (311) of the irradiated sample; d_0 – the value of the lattice period of Al in the plane (311) in the initial state.

Stress σ values can be estimated by the formula:

$$\sigma = \frac{1}{1-\nu}\varepsilon E_\alpha \quad , \qquad (2)$$

where $\nu = 0.330$ is Poisson's coefficient and $E = 7.0 \cdot 10^4$ MPa is Young's modulus.

Data on the value of interplanar distances in the original and irradiated samples of AA1933 alloy were taken from the results of X-ray diffractometry. In the unirradiated sections (311) values of lattice pitch $d_0 =$ 0.12208 nm. In this case, the values of lattice period $d_1 = 0.12213$ in the atomic plane (311) of the irradiated sample. Thus, the XRD results show that a residual stress of about 43 MPa was introduced into the irradiated surface layer. It should be noted that the diffraction peak of the HCPEB-irradiated sample of the studied alloy is shifted toward small angles in comparison with the non-irradiated sample. Based on this, it can be said that it is the tensile macrostresses in the HCPEB-irradiated surface layer that were detected in this study.

During solidification and cooling of the layer melted by HCPEB, there is a partial relaxation of internal stresses resulting from the action of HCPEB. Surface relief of the remelted layer is one of the main sources of information about the primary relaxation mechanisms in the surface irradiated layer. Detailed studies of the surface relief of the irradiated surface of the AA1933 alloy plate were carried out to find out the mechanisms of primary relaxation of internal stresses. An important factor here is that the surface relief of the AA1933 aluminum alloy layer remelted by HCPEB irradiation is very inhomogeneous. Therefore, the study of surface relief features will provide a better understanding of the variety of physical processes occurring during irradiation.

It is known that HCPEB treatment induces strong plastic deformation on the surface of the irradiated sample [10–13]. Plastic deformation during HCPEB irradiation under real conditions often appears as an unintentional process leading to initial stress relaxation induced by the temperature gradient. Thus, the study of the type of surface relief can largely shed light on questions regarding the mechanisms of deformation induced by the action of HCPEB.

Fig. 4 shows micrographs of some fragments of the surface of the studied AA1933 alloy after HCPEB treatment. Such surface morphology of the treated sample is caused by rapid heating, melting, and subsequent crystallization and rapid cooling. First of all, this figure shows a fine and equiaxed granular structure with a grain size of approximately 5 μm. The formation of this microstructure is induced by HCPEB treatment since in the initial state the alloy has a coarser-grained and unequal grain microstructure. It is commonly claimed [1, 2] that HCPEB treatment results in the formation of very fine (1…2 μm) and sometimes nanocrystalline grain microstructure. However, this is not always the case. There are several studies that show that after HCPEB-irradiation a rather coarse-grained grain microstructure was formed in the surface layer. So in [25] on the example of aluminum alloy AA2024 and a number of nickel-based alloys it is shown that the rapid solidification process occurring during surface treatment by HCPEB does not necessarily lead to the formation of nano- or ultrafine grains. Depending on the number of pulses, the grain sizes can even be several times larger than the thickness of the remelted layer. The formation of very large grains is explained here in terms of epitaxial growth of molten liquid from the substrate followed by anomalous grain growth in the solid state. The study [26] reports the formation of large grains with a diameter of 30…40 μm on the surface of HCPEB-irradiated martensitic stainless steel AISI 420. So far, there is no unambiguous understanding of why grains of about 5 μm in size are observed on the remelted surface of the studied alloy. Perhaps a finer-rooted microstructure is initially formed during the crystallization of the molten layer. However, the grain size of the studied AA1933 alloy slightly increases as a result of collecting recrystallization during cooling of the layer remelted by HCPEB.

The fact of the presence of wedge-shaped pores (some of them are indicated by arrows) on this surface (see Fig. 4,a) draws attention. As is known [27], the passage of deformation by the grain boundary slip mechanism is the cause of the porosity formation observed in Fig. 4,a. Wedge-type cracks result from slip inhibition along boundaries at the junction of three grains. It is the porosity of such morphology that is observed in superplastically deformed materials when grain-boundary slipping is the main deformation mechanism [28–30].

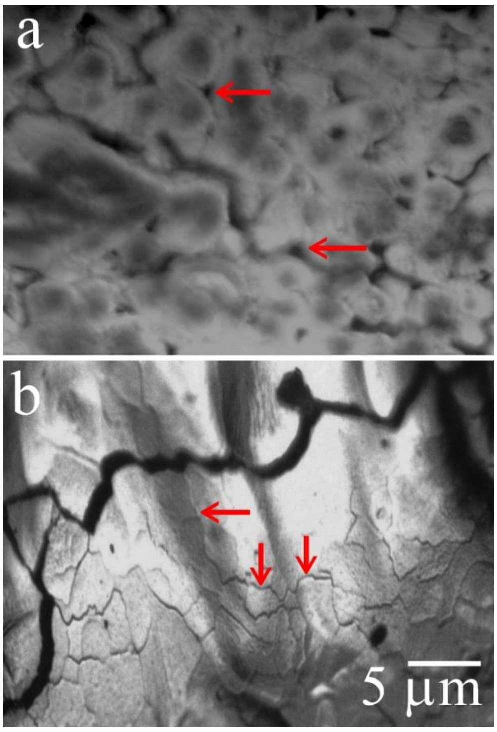

Fig. 4. Characteristic types of microstructure of fragments of irradiated surface of alloy AA1933

Grain-boundary slipping is a high-temperature process. For its realization, grain boundaries must be in an activated state. The presence of local inclusions of liquid phase at grain boundaries may be one of such activated states [31–34]. In the case of AA1933 alloy studied in this paper, such a state can be realized during cooling of the surface layer molten by HCPEB, when due to liquation processes, the inner part of grains will be already crystallized, while the periphery of grains will still be in the liquid state.

A detailed analysis of the relief in Fig. 4, a may suggest that the relaxation of internal stresses can be realized through not just grain-boundary slipping, but the so-called cooperative grain-boundary slipping, which occurs due to the sliding of groups of grains on the surfaces formed by sliding grain boundaries [35]. In Fig. 4,b, the band of possible cooperative grain-boundary slipping is indicated by arrows. That is, we can say that one of the mechanisms of internal stress relaxation during cooling of the layer remelted by HCPEB is exactly grain-boundary slipping or even cooperative grain-boundary slipping. It should also be borne in mind that one of the possible reasons for the formation of surface microcracks may be the inter-granular fracture of the metal occurring at high homologous temperatures at the stage of predominant development of inter-granular deformation. This is the morphology of the inter-granular crack in Fig. 4,b.

A detailed study of the surface relief of the irradiated plate of alloy AA1933 reveals some other features as well. Thus, a close look at the HCPEB-irradiated surface reveals very thin lines on it (Fig. 5). These lines represent marks caused by deformation. In this case, these lines represent dislocation slipping bands (see some of them are marked with arrows in Fig. 5). They are a typical element of the structure of the deformed metal at the dislocation mechanism of deformation. Usually slipping bands on the surface of a deformed specimen are located along the directions of action of maximum shear stresses. A large number of accumulated dislocations is what distinguishes them from the rest of the material. For the band to appear, the initial density of dislocations in the material shall be small and their nucleation must be hindered. Because of this, dislocation slipping is localized near defects that create large overstresses and gradually propagate through the material. It should be noted that dislocation slipping processes in aluminum and alloys based on it are a common and important mechanism of plastic deformation since aluminum is a kind of HCC metal with relatively high energy of packing defects. Thus, observations of the morphology of the irradiated surface show that dislocation slipping is observed in the mechanism of surface layer deformation. However, the density of such lines is not high, which most likely indicates that dislocation slipping is hardly the predominant deformation mechanism, as for example for steels in [10, 11], but is one of the mechanisms, along with other deformation mechanisms.

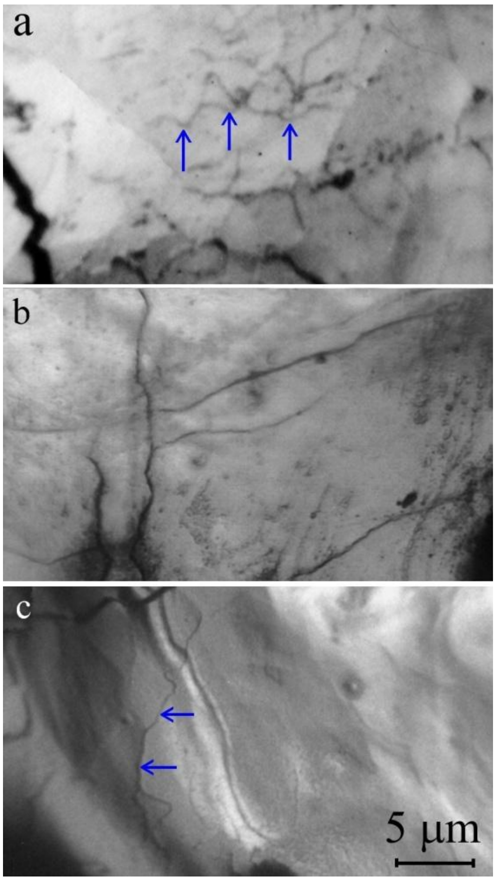

Fig. 5. Characteristic types of microstructure of fragments of irradiated surface of alloy AA1933

CONCLUSIONS

1. Exposure of a pulsed electron beam to a target made of alloy AA1933 leads to the melting of its surface layer. The surface relief of the remelted layer is very inhomogeneous. The formation of relief, which is characterized by the presence of microcracks, craters, and other features indicating the passage of deformation

processes during the cooling of the molten beam surface, occurs on the surface of the remelted layer.

2. X-ray diffraction studies showed that residual tensile internal stresses were present in the surface of the remelted layer. The XRD results show that a residual stress of about 43 MPa was introduced into the irradiated surface layer.

3. Partial relaxation of tensile stresses occurs during the cooling of the molten layer as a result of plastic deformation by several mechanisms. Grain-boundary slipping is one such mechanism for the primary relaxation of internal stresses during the cooling of the layer remelted by HCPEB. Also, according to surface relief observations, plastic deformation during cooling of the surface layer is accomplished by dislocation slipping.

ACKNOWLEDGEMENTS

The research presented in this article was performed by financial support of the Ukrainian state budget program “Support for the development the priority areas of scientific researches” (Budget Financial Code 6541230).

REFERENCES

1. I.N. Onishchenko, V.A. Kiseljob, A.K. Berezin, A.F. Linnik, Ya.B. Fainberg. Wake-field excitation in plasma-dielectric structure by sequence of short bunches of relativistic electrons // *Proceedings of the IEEE Particle Accelerator Conference*. 1995, v. 2, p. 782-783.

2. K.V. Lotov, V.I. Maslov, I.N. Onishchenko. Long sequence of relativistic electron bunches as a driver in wakefield method of charged particles acceleration in plasma // *Problems of Atomic Science and Technology*. 2010, N 6, p. 103-107.

3. D.I. Proskurovsky, V.P. Rotshtein, G.E. Ozur, A.B. Markov, D.S. Nazarov, V.A. Shulov, Y.F. Ivanov, R.G. Buchheit. Pulsed electron-beam technology for surface modification of metallic materials // *J. of Vacuum Sci. and Technol. A*. 1998, v. 16, p. 2480-2488.

4. J.X. Zou, K.M. Zhang, S.Z. Hao, C. Dong, T. Grosdidier, Mechanisms of hardening, wear and corrosion improvement of 316 L stainless steel by low energy high pulsed electron beam surface treatment // *Thin Solid Films*. 2010, v. 519, p. 1404-1415.

5. V.V. Bryukhovetsky, V.F. Klepikov, V.V. Lytvynenko, D.E. Myla, Yu.F. Lonin, A.G. Ponomarev. The Structural Phase State and Strength Properties of the Surface Layer of AA6111-T4 Aluminum Alloy Irradiated by the High-Current Electron Beam // *Nuclear Inst. and Methods in Physics Research B.* 2022, v. 519, p. 1-8.

6. V.V. Bryukhovetsky, A.V. Poyda, V.P. Poyda, D.E. Milaya. Superplastic deformation of the AK4-1 alloy with a surface layer melted by electron pulse beam // *Problems of Atomic Science and Technology*. 2019, N 2(120), p. 67-73.

7. V.V. Bryukhovetsky, V.V. Lytvynenko, D.E. Myla, V.A. Bychko, Yu.F. Lonin, A.G. Ponomarev, V.T. Uvarov. Effect of Structural and Phase Changes under Relativistic Electron Pulsed Beam Irradiation on the Aluminum Alloys Micro-hardness // *Physics and Chemistry of Solid State*. 2021, v. 22, N 4, p. 655-663.

8. D.E. Myla, V.V. Bryukhovetsky, V.V. Lytvynenko, S.I. Petrushenko, O.O. Nevgasimov, Yu.F. Lonin, A.G. Ponomarev, V.T. Uvarov. Microstructure and property modifications in surface layers of a AA6111 aluminum alloy induced by high-current pulsed relativistic electron beam // *Problems of Atomic Science and Technology*. 2022, N 2(138), p. 25-31.

9. K. Zhang, J. Ma, J. Zou, Y. Liu. Surface microstructure and property modifications in a duplex stainless steel induced by high current pulsed electron beam treatments *// Journal of Alloys and Compounds*. 2017, v. 707, p. 178-183.

10. K.M. Zhang, J.X. Zou, B. Bolle, T. Grosdidier. Evolution of residual stress states in surface layers of an AISI D2 steel treated by low energy high current pulsed electron beam // *Vacuum*. 2013, v. 87, p. 60-68.

11. J.X. Zou, K.M. Zhang, T. Grosdidier, C. Dong, Y. Qin, S.Z. Hao, D.Z. Yang. Orientation-dependent deformation on 316L stainless steel induced by high-current pulsed electron beam irradiation // *Mater. Sci. and Eng.: A.* 2008, v. 483-484, p. 302-305.

12. Q.F. Guan, Q.Y. Zhang, C. Dong, G.T. Zou. Deformation twining in single-crystal aluminum induced by high-current pulsed electron beam // *Journal of materials science*. 2005. v. 40, N 18, p. 5049-5052.

13. J. Cai, L. Ji, S.Z. Yang, X.T. Wang, Y. Li, X.L. Hou, Q.F. Guan. Deformation mechanism and microstructures on polycrystalline aluminum induced by high-current pulsed electron beam // *Chinese Science Bulletin*. 2013, v. 58, p. 2507-2511.

14. I.N. Fridlyander. *Aluminum alloys for aerospace engineering. Today, material knowledge of the 21st century*. Kiev: “Naukova dumka”, 1998, 304 p.

15. D.E. Myla, V.V. Bryukhovetsky, V.V. Lytvynenko, V.P. Poyda, A.V. Poyda, V.F. Klepikov, V.T. Uvarov, Yu.F. Lonin, A.G. Ponomarev. Analysis of changes in the phase and structural state of the surface layer of an aluminum alloy 1933, melted by a pulsed electron beam // *Problems of Atomic Science and Technology*. 2020, N 2(126), p. 33-38.

16. V.V. Bryukhovetsky, V.F. Klepikov, V.V. Lytvynenko, D.E. Myla, V.P. Poyda, A.V. Poyda, V.T. Uvarov, Yu.F. Lonin, A.G. Ponomarev. The features of the structural state and phase composition of the surface layer of aluminum alloy Al-Mg-Cu-Zn-Zr irradiated by the high current electron beam // *Nuclear Inst. and Methods in Physics Research B*. 2021, v. 499, p. 25-31.

17. V.P. Poida, D.E. Pedun, V.V. Bryukhovetskii, A.V. Poida, R.V. Sukhov, A.L. Samsonik, V.V. Litvinenko. Structural changes during superplastic deformation of high-strength alloy 1933 of the Al-Mg-Zn-Cu-Zr system // *Phys. Met. Metallogr*. 2013, v. 114, N 9, p. 779-788.

18. Y. Qin, C. Dong, X. Wang, S. Hao, A. Wu, J. Zou, Y. Liu. Temperature profile and crater formation induced in high-current pulsed electron beam processing // *J. Vac. Sci. Tech. A*. 2003, v. 21, N 6, p. 1934-1938.

19. V.V. Bryukhovetsky, V.V. Lytvynenko, Yu.F. Lonin, D.E. Myla, A.G. Ponomarev V.T. Uvarov. Morphological characteristics of craters on the surface of AA1933 aluminum alloy irradiated by pulsed

electron beam // *Problems of Atomic Science and Technology*. 2023, N 2(144), p. 24-28.

20. K. Zhang, J. Zou, T. Grosdidier, C. Dong, D. Yang. Improved pitting corrosion resistance of AISI 316L stainless steel treated by high current pulsed electron beam // *Surf. Coat. Technol*. 2006, v. 201, issue 3-4, p. 1393-1400.

21. Y. Qin, J.X. Zou, C. Dong, X.G. Wang, A.M. Wu, Y. Liu, S. Hao, Q. Guan. Temperature-stress fields and related phenomena induced by a high current pulsed electron beam // *Nucl. Instr. Meth. Phys. Res. B*. 2004, v. 225, issue 4, p. 544-542.

22. V.V. Bryukhovetsky, V.F. Klepikov, V.V. Lytvynenko, D.E. Myla, O.A. Startsev, Yu.F. Lonin, A.G. Ponomarev. Formation mechanism of craters on the surface of AA6111 aluminum alloy irradiated by quasi-relativistic high-current electron beam // *Vacuum*. 2023, v. 215, p. 112263.

23. A.D. Pogrebnjak, A.D. Mikhailov, N.A. Pogrebnjak, Yu.V. Tsvintarnaya, V.I. Lavrentiev, M. Iljashenko, A.N. Valyaev, S. Bratushka, A. Zecca, R. Sandrik. Evolution of vacancy defects and dislocations in surface layers of iron as a result of pulsed electron beam treatment // *Phys. Lett. A*. 1998, v. 241, p. 357-363.

24. A. Taylor and H. Sinclair. On the determination of lattice parameters by the debye-scherrer method // *Proc. Phys. Soc.* 1945, v. 57, N 2, p. 126-145.

25. P. Yan, T. Grosdidier, X. Zhang, and J. Zou. Formation of large grains by epitaxial and abnormal growth at the surface of pulsed electron beam treated metallic samples // *Materials and Design*. 2018, v. 159, p. 1-10.

26. Y. Samih, G. Marcos, N. Stein, N. Allain, E. Fleury, C. Dong, T. Grosdidier. Microstructure modifications and associated hardness and corrosion improvements in the AISI 420 martensitic stainless steel treated by High Current Pulsed Electron Beam (HCPEB) // *Surface and Coatings Technology*. 2014, v. 259, p. 737-745.

27. J. Intrater, E.S. Machlin. Grain boundary sliding and intercrystalline cracking // *Acta Metallurgica*. 1959, v. 7, N 2, p. 140-143.

28. V.V. Bryukhovetskyy, V.P. Pojda, A.V. Poyda, D.R. Avramets', R.I. Kuznetsova, O.P. Kryshtal', O.L. Samsonnik, K.A. Mahmud. Mechanical properties and structural changes during superplastic deformation of 6111 aluminium alloy // *Metallofiz. Noveishie Tekhnol.* 2009, v. 31, issue 9, p. 1289-1302 (in Russian).

29. V.V. Bryukhovetskij. On the origin of high-temperature superplasticity of a coarse-grained avial-type aluminum alloy // *Fizika Metallov i Metallovedenie*. 2001, v. 92, issue 1, p. 107-111 (in Russian).

30. A.V. Pojda, V.V. Bryukhovets'ky, D.L. Voronov, R.I. Kuznetsova, V.F. Klepikov. Superplastic behaviour of an AlMg6 alloy at the high homological temperatures // *Metallofiz. Noveishie Tekhnol.* 2005, v. 27, issue 3, p. 317-330 (in Russian).

31. V.V. Bryukhovetsky, R.I. Kuznetsova, N.N. Zhukov, V.P. Poida, V.F. Klepikov. Liquid-phase nucleation and evolution as a cause of superplasticity in alloys of the Al-Ge system *// Phys. Stat. Sol. (A).* 2005, v. 202, N 9, p. 1740-1750.

32. V.P. Pojda, V.V. Bryukhovets'ky, R.I. Kuznetsova, A.V. Pojda, V.F. Klepikov. Formation and development of the fibre structures during superplastic deformation of matrix aluminium alloys // *Metallofiz. Noveishie Tekhnol.* 2003, v. 25, issue 1, p. 117-132 (in Russian).

33. V.P. Poida, V.V. Bryukhovetskii, A.V. Poida, R.I. Kuznetsova, V.F. Klepikov, D.L. Voronov. Morphology and mechanisms of the formation of fiber structures upon high-temperature superplastic deformation of aluminum alloys // *Phys. Met. Metallogr*. 2007, v. 103, N 4, p. 414-423.

34. V.V. Bryukhovetskii, V.P. Poida, A.V. Poida, R.I. Kuznetsova, K.A. Mahmoud, D.E. Pedun. Phase transformations and structural changes in the course of the high-temperature superplastic deformation of aluminum alloys // *Phys. Met. Metallogr*. 2010. v. 110, N 6, p. 588-596.

35. V.V. Astanin, O.A. Kaibyshev, S.N. Faizova. Cooperative grain boundary sliding under superplastic flow // *Scripta Met. at Mater*. 1991, v. 25, N 12, p. 2663-2668.

Article received 01.02.2024

ЗАЛИШКОВІ НАПРУЖЕННЯ ТА МЕХАНІЗМИ ДЕФОРМАЦІЇ У ПОВЕРХНЕВОМУ ШАРІ АЛЮМІНІЄВОГО СПЛАВУ АА1933, ВИКЛИКАНІ ОПРОМІНЕННЯМ СИЛЬНОСТРУМОВИМ ІМПУЛЬСНИМ ЕЛЕКТРОННИМ ПУЧКОМ

В.В. Брюховецький, В.В. Литвиненко, Д.Є. Мила, В.В. Шатов, А.Г. Пономарьов, О.Л. Рак, В.А. Бичко

Метою цієї роботи було з'ясувати і показати, що швидке затвердіння поверхневого шару алюмінієвого сплаву АА1933, розплавленого опроміненням високострумового імпульсного пучка електронів, призводить до розвитку у цьому шарі деформаційних процесів. Це є результатом дії термопружних внутрішніх напружень, що виникають при опроміненні сплаву імпульсним пучком електронів. Встановлено, що величина залишкових внутрішніх напружень у переплавленому опроміненням поверхневому шарі становить 43 МПа. Оскільки прямими методами механізми деформації у ході остигання переплавленого шару визначити неможливо, висновки про механізми деформації робили шляхом дослідження рельєфу опроміненої поверхні. У роботі продемонстровано, що деформаційні процеси при опроміненні алюмінієвого сплаву АА1933 можуть розвиватися у різних ділянках опроміненої поверхні за різними механізмами. Деформація може здійснюватися як за механізмами дислокаційного ковзання, так і за механізмом зернограничного проковзування.